Mendeleev Communications

Mendeleev Commun., 2025, **35**, 390–392

Fullerene-based carboxylic acids for improving performance and stability of perovskite solar cells

Olga A. Kraevaya,*[a] Sergey L. Nikitenko,[a] Nikita A. Slesarenko,[a] Evgeniya P. Antoshkina,[b,c] Ekaterina A. Khakina,[b] Alexander S. Peregudov,[b] Pavel A. Troshin[d,a] and Sergey M. Aldoshin[a]

[a] *Federal Research Center of Problems of Chemical Physics and Medicinal Chemistry, Russian Academy of Sciences, 142432 Chernogolovka, Moscow Region, Russian Federation. E-mail: okraevaya@inbox.ru*
[b] *A. N. Nesmeyanov Institute of Organoelement Compounds, Russian Academy of Sciences, 119334 Moscow, Russian Federation*
[c] *Moscow Institute of Physics and Technology (National Research University), 141701 Dolgoprudny, Moscow Region, Russian Federation*
[d] *Zhengzhou Research Institute, Harbin Institute of Technology, 450003 Zhengzhou, China*

DOI: 10.71267/mencom.7688

We report a family of fullerene-based carboxylic acids with varied molecular structure affecting their ability to anchor to the surface of metal oxides, in particular SnO_2, used as electron-transport materials in n-i-p perovskite solar cells. Compounds having the lowest solubility and/or increased number of carboxyl groups per fullerene core tend to form more robust passivation coatings over SnO_2 and thus deliver the highest solar cell efficiencies and the best device operational stabilities. The results indicate the promise of further rational design of the fullerene-based acids with improved properties to achieve simultaneously a high solar light conversion efficiency and a long-term stability.

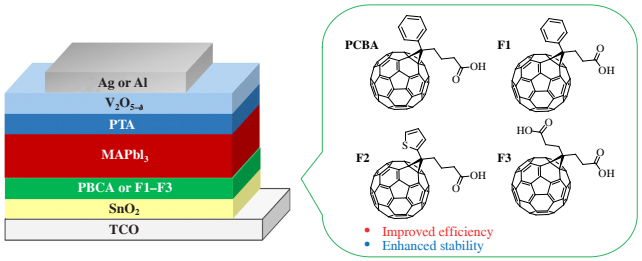

Keywords: fullerene derivatives, electron-transport materials, perovskite solar cells, stability, passivation coatings.

Organic and perovskite solar cells (OSCs and PSCs, respectively) represent rapidly emerging photovoltaic technologies, which are already entering the commercialization stage and can be not only used in some niche applications, such as textile- or building-integrated systems, but also finally compete with conventional silicon panels in grid-connected solar power plants. The record-breaking certified efficiencies of small-area OSCs and PSCs approach 19.2 and 26.7%, respectively, which are very close to those of the best crystalline Si solar cells (27.3%).[1] This rapid progress in the efficiency of new photovoltaic technologies is associated with innovations in materials, mainly new absorbers for OSCs and charge-transport materials for PSCs.[2,3] However, in the context of improving operational stability of both types of devices, the development of new hole-transport and electron-transport materials forming defect-free interfaces with absorber layers is currently the major research paradigm.[4,5]

Historically, titanium dioxide was one of the first electron-transport layer materials stemming from research on dye sensitized solar cells.[6] However, the high chemical activity of TiO_2 surface leading to fast device degradation[7] motivated an intense search for more stable interfacial materials, mainly ZnO for organic solar cells[8] and SnO_2 for perovskite devices.[9,10] The application of these oxide electron-transport layers considerably enhanced the efficiency and stability of OSCs and PSCs.[4,11] However, the problem of interfacial degradation was not completely solved; therefore, different passivation coatings deposited at the oxide electron-transport layer (ETL)/absorber interfaces have been intensively developed for both OSCs and PSCs.[12–15]

Fullerene derivatives[16] are highly popular electron-transport materials for organic and perovskite solar cells.[17–21] Previously, we used fullerene-based phenyl-C_{61}-butyric acid (PCBA) as a passivation coating for SnO_2, which significantly enhanced photovoltaic performance and also improved the stability of n-i-p PSCs as compared to the devices based on bare tin dioxide ETL.[22] More recently, a broader range of fullerene-based acids has been explored, and compounds with one or two carboxyl groups attached to the fullerene cage within a single compact-size organic addend were found to be the most promising.[23] However, the operational stability of PSCs using all of the designed fullerene-based passivation coatings was very similar and not sufficient for practical implementation. Herein, we have rationally designed three new fullerene-based carboxylic acids in order to determine the effects of the molecular structure of these compounds on the efficiency and, most importantly, operational stability of PSCs.

Fullerene-based acids **F1**–**F3** were synthesized with almost quantitative yields starting from corresponding ester compounds **1**–**3**[24] using a mixture of acetic and hydrochloric acids for ester group cleavage (Scheme 1). The molecular structures of the fullerene derivatives were confirmed by MALDI ToF mass spectrometry and 1D and 2D NMR spectroscopy (Online Supplementary Materials, Figures S1–S18). The compounds demonstrated very low solubility in organic solvents due to intermolecular hydrogen bonding effects. **F1** and **F2** were dissolved in chlorobenzene to form 0.1 mg ml^{-1} solutions, while **F3**, possessing two carboxyl groups, was solubilized

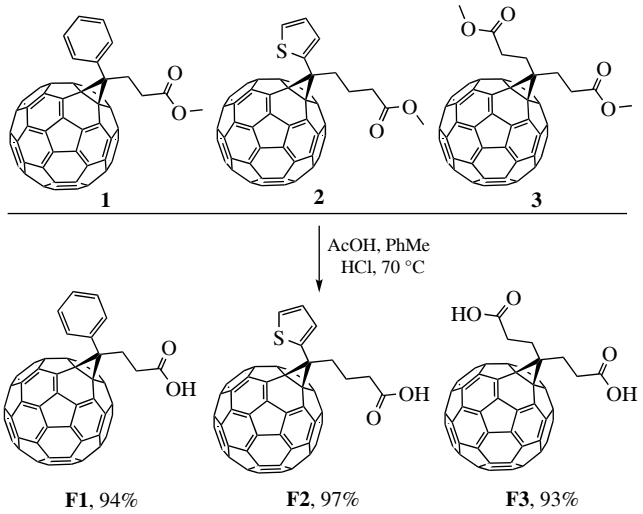

Scheme 1 Synthesis of fullerene-based carboxylic acids **F1–F3**.

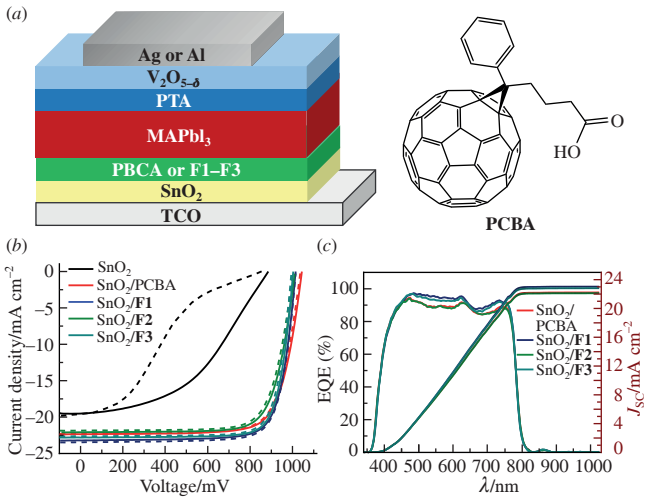

Figure 1 (*a*) Schematic layout of the n-i-p PSC architecture. (*b*) Reverse (solid lines) and forward (dashed lines) scan *J*–*V* curves and (*c*) EQE spectra of PSCs assembled using bare or modified SnO_2 with fullerene-based carboxylic acids.

only in a CS_2–THF mixture (83 : 17, v/v) to reach the above concentration.

Compounds **F1–F3** were deposited on the oxide electron-transport layer either by spin coating of fullerene derivative solutions at a high frequency (3000–3500 rpm) or by soaking the SnO_2 films in solutions of the fullerene derivatives for 1 h. The surface properties of SnO_2/fullerene derivative films prepared by the two different methods were comparable. The water contact angle increased dramatically from 19.2° for unmodified SnO_2 to 55–65° after coating **F1–F3** or even up to 74° when soaking in a PCBA solution. Consequently, the total surface energy decreased from about 74 to 53–58 mN m^{-1} (Online Supplementary Materials, Table S1). These results clearly indicate that the surface of SnO_2 was modified by fullerene derivatives **F1–F3** similarly to PCBA. Thus, the carboxyl groups enabled efficient anchoring of the fullerene derivatives to the oxide surface.

The electrical performance of the SnO_2 films modified by the fullerene derivatives has been explored in n-i-p perovskite solar cells assembled in the glass/ITO/SnO_2/fullerene derivative/$MAPbI_3$/PTA/$V_2O_{5-\delta}$/Ag configuration, where ITO is an indium–tin oxide transparent electrode, $MAPbI_3$ is a methylammonium iodoplumbate perovskite absorber, PTA is poly[bis(4-phenyl)(4-methylphenyl)amine][25] used as a hole-transport layer material, and oxygen-deficient $V_2O_{5-\delta}$ forms an electron-blocking and diffusion barrier coating under the top metal electrode.[26] The silver top electrode was routinely used to evaluate the device performance, whereas we applied aluminum electrodes for stability tests since they have a reduced tendency to diffuse into the inner part of the device under harsh solar cell operational conditions. Figure 1(*a*) shows a schematic diagram of the device.

Preliminary experiments showed that the performances of PSCs with the fullerene-based passivation coatings deposited by soaking and spin-coating are very comparable, with slightly better results obtained using the latter approach. Therefore, we continued device optimization using the spin-coating process for the deposition. The results are presented in Table 1. The current–voltage (*J*–*V*) characteristics of the best performing solar cells of each type are shown in Figure 1(*b*), while their external quantum efficiency (EQE) spectra are given in Figure 1(*c*).

The results emphasized the importance of the fullerene-based passivation coatings since the PSCs fabricated using bare SnO_2 showed very poor PCE values of <8% and extremely high hysteresis in *J*–*V* characteristics. On the contrary, all PSCs with the fullerene-based passivation coatings showed more than twice higher efficiencies with negligible hysteresis. Fullerene

Table 1 Characteristics of PSCs assembled using fullerene-based passivation coatings.[a]

ETL	V_{OC}/mV	J_{SC}/ mA cm^{-2}	J_{SC}^{EQE}/ mA cm^{-2}	FF (%)[b]	PCE (%)
F1	1011.5 (995.7 ± 17.2)	23.3 (22.8 ± 0.5)	23.1	77.6 (75.4 ± 3.7)	18.3 (17.2 ± 1.1)
F2	1005.6 (1006.4 ± 14.6)	22.2 (21.5 ± 0.8)	22.1	76.4 (73.1 ± 5.1)	17.1 (15.8 ± 1.2)
F3	1003.7 (991.2 ± 15.3)	22.9 (22.6 ± 0.5)	22.8	79.2 (77.1 ± 2.1)	18.2 (17.3 ± 0.9)
PCBA	1044.1 (1033.2 ± 10.8)	22.3 (22.1 ± 0.4)	22.2	75.7 (73.4 ± 2.9)	17.6 (16.7 ± 0.9)
SnO_2	986.5 (906.4 ± 80.1)	19.7 (18.7 ± 1.1)		45.4 (37.2 ± 8.2)	7.9 (6.3 ± 1.6)

[a]Data extracted from reverse-scan *J*–*V* characteristics. [b]FF – fill factor of the solar cell.

derivatives **F1** and **F3** enabled the best performance characteristics with power conversion efficiency (PCE) values of >18% (see Table 1). The PSCs assembled with **F2** delivered slightly lower PCE values (17.1%) than reference devices fabricated using PCBA (17.6%).

Note that fullerene derivatives **F1** and **F3** have the lowest solubility in organic solvents and the highest tendency to crystallize, which can be a prerequisite for their advanced performance in PSCs. Indeed, the self-assembled monolayer of a fullerene-based acid deposited on the SnO_2 surface should be very compact and highly ordered to support efficient electron extraction and transfer into the oxide-based ETL. Furthermore, it should be resistant to solvent treatment and sustain the deposition of a perovskite absorber layer from the *N*,*N*-dimethylformamide (DMF)–*N*-methylpyrrolidone (NMP) solvent mixture.

The operational stability of PSCs was investigated in an inert atmosphere inside a glove box to simulate ideal device encapsulation conditions. Therefore, all the observed aging effects should be considered intrinsic and attributed to the evolution of functional layers and interfaces under the light and heat stress. The cells were illuminated with white light (100 mW cm^{-2}) under open-circuit conditions to dramatically accelerate the degradation of PSCs.[27] The equilibrium surface temperature of the devices was 40–50 °C, which means that $MAPbI_3$ or other device components should not undergo heat-induced degradation in the bulk.

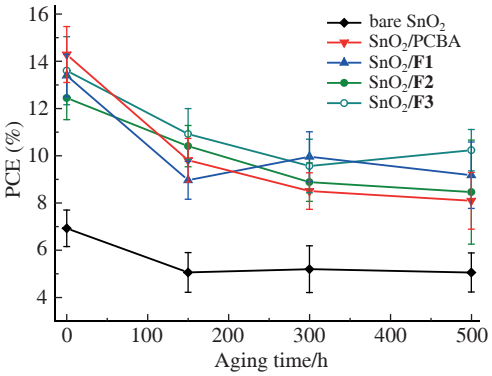

Figure 2 Evolution of the power conversion efficiency of PSCs using different ETL materials and Al top electrodes under continuous exposure to white light under open-circuit conditions. The statistics were obtained from at least 25 cells in each series.

Figure 2 shows the evolution of the PSC characteristics within 500 h of continuous light exposure. The reference devices with PCBA passivation coating were the least stable and lost >40% of their initial PCE value by the end of the aging tests. The highest stability was exhibited by PSCs assembled with **F3** and **F1**, whereas the devices using **F2** as a passivation coating behaved similarly to the reference cells with PCBA. Thus, there was a clear relationship between the device efficiency and operational stability. We believe that fullerene derivatives **F1** and **F3** formed the densest and most robust self-assembled monolayers on the surface of SnO_2, making it inaccessible to direct interactions with a perovskite absorber layer leading to the interface failure. On the contrary, PCBA and **F2** were more labile on the SnO_2 surface and migrated into the bulk of the absorber layer, thus facilitating perovskite/SnO_2 interface degradation.

Thus, we synthesized a family of fullerene-based carboxylic acids and evaluated their performance as passivation coatings for SnO_2 ETLs in n-i-p PSCs. Two fullerene derivatives improved photovoltaic performance and, most importantly, also operational stability of PSCs in comparison with the reference cells using PCBA as a passivation coating. The fullerene derivatives capable of effective anchoring to the oxide surface and formation of robust coatings can deliver simultaneously a high photovoltaic efficiency and a long-term device operational stability. The rational molecular engineering of the fullerene-based passivation coatings should be focused on increasing their interactions with the oxide surface and preventing degradation of self-assembled monolayers during the subsequent deposition of the perovskite absorber layer.

This work was supported by the Russian Ministry of Science and Higher Education (grant no. 075-15-2022-1216). The contribution of Center for molecule composition studies of INEOS RAS is gratefully acknowledged.

Online Supplementary Materials

Supplementary data associated with this article can be found in the online version at doi: 10.71267/mencom.7688.

References

1 M. A. Green, E. D. Dunlop, M. Yoshita, N. Kopidakis, K. Bothe, G. Siefer, D. Hinken, M. Rauer, J. Hohl-Ebinger and X. Hao, *Prog. Photovoltaics*, 2024, **32**, 425; https://doi.org/10.1002/pip.3831.
2 M. Li and F. He, *Next Energy*, 2024, **2**, 100085; https://doi.org/10.1016/j.nxener.2023.100085.
3 C. Yang, W. Hu, J. Liu, C. Han, Q. Gao, A. Mei, Y. Zhou, F. Guo and H. Han, *Light: Sci. Appl.*, 2024, **13**, 227; https://doi.org/10.1038/s41377-024-01461-x.
4 P. Ding, D. Yang, S. Yang and Z. Ge, *Chem. Soc. Rev.*, 2024, **53**, 2350; https://doi.org/10.1039/D3CS00492A.
5 H. Zhu, S. Teale, M. N. Lintangpradipto, S. Mahesh, B. Chen, M. D. McGehee, E. H. Sargent and O. M. Bakr, *Nat. Rev. Mater.*, 2023, **8**, 569; https://doi.org/10.1038/s41578-023-00582-w.
6 K. Sharma, V. Sharma and S. S. Sharma, *Nanoscale Res. Lett.*, 2018, **13**, 381; https://doi.org/10.1186/s11671-018-2760-6.
7 Q. Fatima, A. A. Haidry, H. Zhang, A. El Jery and M. Aldrdery, *Mater. Today Sustainability*, 2024, **27**, 100857; https://doi.org/10.1016/j.mtsust.2024.100857.
8 Y. Wang, Z. Zheng, J. Wang, X. Liu, J. Ren, C. An, S. Zhang and J. Hou, *Adv. Mater.*, 2023, **35**, 2208305; https://doi.org/10.1002/adma.202208305.
9 S. Y. Park and K. Zhu, *Adv. Mater.*, 2022, **34**, 2110438; https://doi.org/10.1002/adma.202110438.
10 Q. Wali, M. Aamir, M. E. Khan, R. Jose, W. Fan and S. Yang, *Sol. Energy*, 2024, **270**, 112382; https://doi.org/10.1016/j.solener.2024.112382.
11 N. Ren, L. Tan, M. Li, J. Zhou, Y. Ye, B. Jiao, L. Ding and C. Yi, *iEnergy*, 2024, **3**, 39; https://doi.org/10.23919/IEN.2024.0001.
12 Q. Ye, Y. Zhao, S. Mu, F. Ma, F. Gao, Z. Chu, Z. Yin, P. Gao, X. Zhang and J. You, *Adv. Mater.*, 2019, **31**, 1905143; https://doi.org/10.1002/adma.201905143.
13 Z. Wu, J. Su, N. Chai, S. Cheng, X. Wang, Z. Zhang, X. Liu, H. Zhong, J. Yang, Z. Wang, J. Liu, X. Li and H. Lin, *Adv. Sci.*, 2023, **10**, 2300010; https://doi.org/10.1002/advs.202300010.
14 M. Guli, Y. Zhang, R. Li, W. He, C. Lan and Y. Zhou, *Nano Lett.*, 2024, **24**, 14183; https://doi.org/10.1021/acs.nanolett.4c02824.
15 J. Wu, F. Tang, S. Wu, Y. Li, L. Xiao, X. Zhu and X. Peng, *Adv. Energy Mater.*, 2024, **14**, 2302932; https://doi.org/10.1002/aenm.202302932.
16 O. A. Kraevaya, A. V. Chernyak, A. F. Shestakov and P. A. Troshin, *Mendeleev Commun.*, 2024, **34**, 411; https://doi.org/10.1016/j.mencom.2024.04.032.
17 C. Gong, H. Li, Z. Xu, Y. Li, H. Wang, Q. Zhuang, A. Wang, Z. Li, Z. Guo, C. Zhang, B. Wang, X. Li and Z. Zang, *Nat. Commun.*, 2024, **15**, 9154; https://doi.org/10.1038/s41467-024-53283-5.
18 U. Ali, S. Javed, A. A. Qureshi and M. A. Akram, *ChemNanoMat*, 2023, **9**, e202300175; https://doi.org/10.1002/cnma.202300175.
19 H. Sun, K. Xiao, H. Gao, C. Duan, S. Zhao, J. Wen, Y. Wang, R. Lin, X. Zheng, H. Luo, C. Liu, P. Wu, W. Kong, Z. Liu, L. Li and H. Tan, *Adv. Mater.*, 2024, **36**, 2308706; https://doi.org/10.1002/adma.202308706.
20 S. Zeng, H. Wang, X. Li, H. Guo, L. Dong, C. Guo, Z. Chen, J. Zhou, Y. Sun, W. Sun, L. Yang, W. Li, D. Liu and T. Wang, *J. Energy Chem.*, 2025, **102**, 172; https://doi.org/10.1016/j.jechem.2024.10.046.
21 E. Hou, S. Cheng, Y. Qiu, X. Chen, J. Chen, C. Sun, H. Zhang, J. Yang, X. Zhao, L. Xie, Z. Chen, C. Tian and Z. Wei, *Angew. Chem., Int. Ed.*, 2024, e202416703; https://doi.org/10.1002/anie.202416703.
22 S. Tsarev, T. S. Dubinina, S. Yu. Luchkin, I. S. Zhidkov, E. Z. Kurmaev, K. J. Stevenson and P. A. Troshin, *J. Phys. Chem. C*, 2020, **124**, 1872; https://doi.org/10.1021/acs.jpcc.9b10709.
23 A. F. Akbulatov, O. A. Kraevaya, V. S. Bolshakova, L. A. Frolova and P. A. Troshin, *Synth. Met.*, 2023, **299**, 117468; https://doi.org/10.1016/j.synthmet.2023.117468.
24 P. A. Troshin, H. Hoppe, J. Renz, M. Egginger, J. Yu. Mayorova, A. E. Goryachev, A. S. Peregudov, R. N. Lyubovskaya, G. Gobsch, N. S. Sariciftci and V. F. Razumov, *Adv. Funct. Mater.*, 2009, **19**, 779; https://doi.org/10.1002/adfm.200801189.
25 S. Tsarev, I. K. Yakushchenko, S. Yu. Luchkin, P. M. Kuznetsov, R. S. Timerbulatov, N. N. Dremova, L. A. Frolova, K. J. Stevenson and P. A. Troshin, *Sustainable Energy Fuels*, 2019, **3**, 2627; https://doi.org/10.1039/C9SE00448C.
26 M. M. Tepliakova, A. N. Mikheeva, L. A. Frolova, A. G. Boldyreva, A. Elakshar, A. V. Novikov, S. A. Tsarev, M. I. Ustinova, O. R. Yamilova, A. G. Nasibulin, S. M. Aldoshin, K. J. Stevenson and P. A. Troshin, *J. Phys. Chem. Lett.*, 2020, **11**, 5563; https://doi.org/10.1021/acs.jpclett.0c01600.
27 K. Domanski, E. A. Alharbi, A. Hagfeldt, M. Grätzel and W. Tress, *Nat. Energy*, 2018, **3**, 61; https://doi.org/10.1038/s41560-017-0060-5.

Received: 21st November 2024; Com. 24/7688